

Extreme synchronization events in a Kuramoto model: The interplay between resource constraints and explosive transitions

Cite as: Chaos 31, 063103 (2021); <https://doi.org/10.1063/5.0055156>

Submitted: 26 April 2021 . Accepted: 17 May 2021 . Published Online: 01 June 2021

 Nikita Frolov, and  Alexander Hramov

COLLECTIONS

Paper published as part of the special topic on [In Memory of Vadim S. Anishchenko: Statistical Physics and Nonlinear Dynamics of Complex Systems](#)



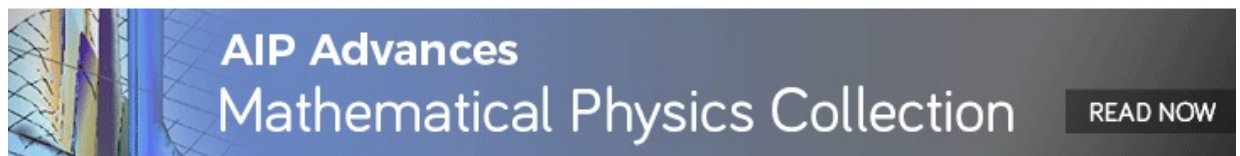
View Online



Export Citation



CrossMark



Extreme synchronization events in a Kuramoto model: The interplay between resource constraints and explosive transitions

Cite as: Chaos 31, 063103 (2021); doi: 10.1063/5.0055156

Submitted: 26 April 2021 · Accepted: 17 May 2021 ·

Published Online: 1 June 2021



View Online



Export Citation



CrossMark

Nikita Frolov^{1,2,a)}  and Alexander Hramov^{1,2,b)} 

AFFILIATIONS

¹Neuroscience and Cognitive Technology Laboratory, Center for Technologies in Robotics and Mechatronics Components, Innopolis University, 420500 Innopolis, The Republic of Tatarstan, Russia

²Center for Neurotechnology and Machine Learning, Immanuel Kant Baltic Federal University, 236041 Kaliningrad, Russia

Note: This paper is part of the Focus Issue, In Memory of Vadim S. Anishchenko: Statistical Physics and Nonlinear Dynamics of Complex Systems.

^{a)}Author to whom correspondence should be addressed: n.frolov@innopolis.ru

^{b)}Electronic mail: hramovae@gmail.com

ABSTRACT

Many living and artificial systems possess structural and dynamical properties of complex networks. One of the most exciting living networked systems is the brain, in which synchronization is an essential mechanism of its normal functioning. On the other hand, excessive synchronization in neural networks reflects undesired pathological activity, including various forms of epilepsy. In this context, network-theoretical approach and dynamical modeling may uncover deep insight into the origins of synchronization-related brain disorders. However, many models do not account for the resource consumption needed for the neural networks to synchronize. To fill this gap, we introduce a phenomenological Kuramoto model evolving under the excitability resource constraints. We demonstrate that the interplay between increased excitability and explosive synchronization induced by the hierarchical organization of the network forces the system to generate short-living extreme synchronization events, which are well-known signs of epileptic brain activity. Finally, we establish that the network units occupying the medium levels of hierarchy most strongly contribute to the birth of extreme events emphasizing the focal nature of their origin.

Published under an exclusive license by AIP Publishing. <https://doi.org/10.1063/5.0055156>

Studying the synchronization in complex networks capturing the properties of neuronal populations is crucial for understanding the brain's functioning in normal and pathological conditions. The latter implies insights into the origins of excessive neuronal synchronization, its prediction, and complete or partial suppression. To duly address these issues through dynamical modeling, one should account for the fact that the neuronal ensembles synchronize under limited resource constraints. With this aim, we develop a network model evolving under the consumption of excitability resources. Our proposed model exhibits the generation of extreme synchronization events at increased excitability and topology-induced explosive transitions. We demonstrate that the origination of extreme synchronization events on the microscopic level is subserved by the medium-degree units, which we refer to as “influential” nodes. Importantly, our phenomenological model, despite its simplicity, reflects several

properties of epileptic seizures known from prior physiological studies.

I. INTRODUCTION

Professor Vadim Anishchenko was one of the founding fathers of such a scientific direction as nonlinear dynamics and the theory of dynamic chaos both at Saratov University and throughout Russia. For the first time in 1990, he published a pioneering book *Complex Oscillations in Simple Systems*¹ on dynamic chaos in Russia. In this book, he studied the chaos in a generator with inertial nonlinearity, which was later called the Anishchenko–Astakhov generator. Professor Anishchenko's scientific interests in this area were extensive—from problems of the theory of bifurcations to the application of methods of nonlinear dynamics to the analysis

of biological systems.² In recent years, Vadim Anishchenko has been actively involved in such a new and promising scientific field as the theory of complex networks, including the study of subtle effects, leading to the formation of chimera states. In this direction, Professor Anishchenko and his research team have made many exciting studies. In particular, he, together with his bright colleague Dr. Galina Strelkova, investigated chimeras in ensembles of chaotic oscillators.^{3–5} In this paper, we consider an issue that closely coincides with the last studies of Professor Vadim Anishchenko, namely, the formation of synchronous states in a network of phase oscillators with certain modifications of the oscillator model. For all of us, his students, colleagues, and friends, his death was a huge loss.

Many living and man-made systems possess structural and dynamical properties of complex networks.⁶ A synchronization is an essential mechanism underlying normal functioning of biological,^{7,8} physiological,^{9–11} social,¹² electrical systems,^{13,14} etc. One of the most fascinating living networked systems is the brain, in which synchronization is vital in the coordination of distributed neural networks, transmission, and encoding of information.^{15–17} On the other hand, an excessive synchronization in neural networks reflects undesired and hazardous aspects of collective behavior, including various forms of epilepsy^{18–21} and Parkinson's disease.²²

In this context, network science and dynamical modeling offer a rich methodological background to gain a deeper understanding of the pathological aspects of collective behavior in neural networks. Biologically inspired network models have been proposed and analyzed in the works by Medvedeva *et al.*^{23,24} Lehnertz and co-workers have explored complex dynamics behind spatiotemporal patterns^{25,26} and extreme behavior^{27,28} in excitable media. Recently, Schöll and co-workers have addressed the impact of the network topology on epileptic-seizure-related synchronization.²⁹

Importantly, brain neural networks synchronize under limited resource consumption. The ability of neuronal ensembles to produce a coherent response is determined by the excitability of individual neurons, i.e., the capacity of ion channels.³⁰ There is a view that an increased neuronal excitability underlies a development of the pathological brain states and is caused by a mutation of molecular constituents of neural networks.³¹ Thus, the account of resource consumption is vital in development of relevant models of neuronal interactions.

Recently, several network models evolving under resource constraints have been developed. Kroma-Wiley *et al.* have studied synchronization in coupled Kuramoto oscillators, where resource consumption and production are a function of their angular velocity.³² They demonstrate that, along with trivial globally coherent and incoherent states, the system exhibits partial synchronization with either an oscillating order parameter or the coexistence of multiple synchronized states. Also, Zhang and Strogatz have designed a temporal network under a limited coupling budget.³³ The authors show that the proposed time-varying model synchronizes more efficiently than optimal static networks.

In the current work, we propose a model of collective dynamics under excitability resource constraints. Using an extensive numerical simulation, we demonstrate that under the interplay between explosive synchronization (ES) and an increased excitability resource, our model exhibits extreme behavior—an important attribute of epileptic-seizure-related activity.^{34–37} We

suggest that ES would support an abrupt transition to coherence, while a decay of resource would terminate a synchronous state. Although many potential mechanisms lead to explosive transitions in complex networks,³⁸ we restrict our analysis to the ES induced by the hierarchical network organization.³⁹

The paper is organized as follows. Section II describes a proposed Kuramoto model under the excitability resource constraints. Section III reports the main findings of our study including macroscopic properties of extreme synchronization in the Kuramoto network and its association with microscopic dynamics. Section IV summarizes and discusses the obtained results in terms of the prior neurophysiological studies.

II. MODEL

A conventional Kuramoto model comprises N interacting phase oscillators as sketched in Fig. 1(a), and the dynamics of each oscillator is governed by the following equation:

$$\dot{\theta}_i = \omega_i + \lambda \sum_{j=1}^N \mathcal{A}_{ij} \sin(\theta_j - \theta_i). \quad (1)$$

Here, θ_i and $\dot{\theta}_i$ are the phase and angular velocity of the i th oscillator, $i \in [1, N]$, ω_i is its natural frequency, and λ is a coupling strength. Connections of the network are defined by the adjacency matrix \mathcal{A} , in which $\mathcal{A}_{ij} = 1$ determines the presence of a link between the i th and j th nodes, and the link is absent if $\mathcal{A}_{ij} = 0$. Local synchrony in the neighborhood of the i th oscillator is estimated by the local order parameter $r_i = 1/k_i \left| \sum_{j=1}^N \mathcal{A}_{ij} e^{i\theta_j} \right|$, where $k_i = \sum_{j=1}^N \mathcal{A}_{ij}$ defines the i th node's degree. Global coherence is quantified using a global order parameter $R = 1/N \left| \sum_{j=1}^N e^{i\theta_j} \right|$.

We consider phase oscillators having degree-dependent natural frequencies such that $\omega_i = k_i$. This assumption is relevant for a class of real networked systems, including power grids and, particularly, neural networks, and is an essential condition for establishing explosive transitions in several types of network topology.

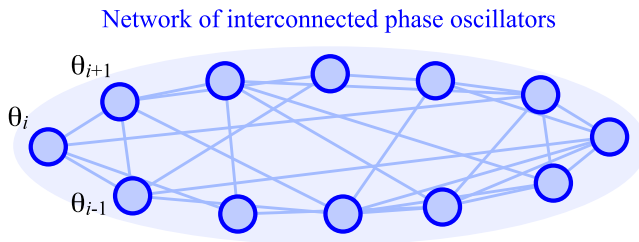
A coupling strength λ being the only parameter controlling the transition to coherence in Eq. (1) could be interpreted as excitability of the ensemble. In many man-made and living networked systems, excitability could not be set constant and equal for all nodes. Moreover, the excitability could not be maintained during prolonged periods of coherence due to a limitation of the system's resources. The proposed model accounts for the time-varying nature of excitability of individual units by their connection to resource baths λ_i through a diffusive coupling [Fig. 1(b)]. Here, the excitability consumption is considered a function of the local order parameter r_i . A conventional Kuramoto model is, therefore, modified in the following way:

$$\dot{\theta}_i(t) = \omega_i + \lambda_i(t) \sum_{j=1}^N \mathcal{A}_{ij} \sin(\theta_j(t) - \theta_i(t)), \quad (2)$$

$$\dot{\lambda}_i(t) = \alpha(\lambda_i(t) - \lambda_0) - \beta r_i(t). \quad (3)$$

The first term in the right-hand side of Eq. (3) implies the excitability recovery at a rate α , while the second term accounts for

(a) Conventional Kuramoto model



(b) Kuramoto model under resource constraints

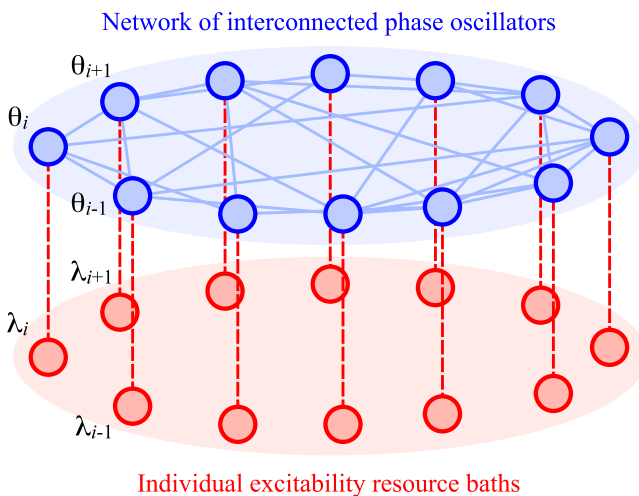


FIG. 1. Model under study. (a) Illustration of a conventional Kuramoto model. Here, N oscillators (blue circles), whose state is defined by phase θ_i , $i \in [1, N]$, are interacting through the connections presented with blue solid lines. (b) Illustration of the proposed Kuramoto model under resource constraints, which implies that each network's unit is connected to an individual resource bath (red circles) through a diffusive coupling (red dashed lines). The level of resource bath defines the excitability λ_i of an individual phase oscillator.

the resource constraints at a rate β . λ_0 is an unperturbed level of excitability in the absence of resource constraints, i.e., at $\beta = 0.0$. In other words, it defines the depth of an individual resource bath and is set identical for all units. In the current study, we explore the dynamics of a system governed by Eqs. (2) and (3) controlled by λ_0 , while parameters α and β remain fixed. Here, slow resource consumption at a rate $\beta = 0.002$ is contrasted by a fast resource recovery at a rate $\alpha = 0.01$.

III. RESULTS AND DISCUSSION

In the current study, the dynamics of Kuramoto networks are explored through the extensive numerical simulations fully conducted in Julia language using a `DifferentialEquations` solver.⁴⁰ Specifically, we integrate Eqs. (1)–(3) for $N = 10^3$ units using the fourth-order Runge–Kutta (RK4) algorithm with adaptive time-stepping and keep the relative tolerance equal to 10^{-4} . This

numerical algorithm is chosen due to the instability of a fixed time-stepping RK4 method concerning the degree-dependent natural frequencies of interacting oscillators.

To observe rare extreme events of synchronization, we simulate network dynamics on a large timescale, namely, $t \in [0, 10^5]$ time units. To address the impact of topology, we consider networks whose coupling architecture is given by the random small-world (SW) and hierarchical scale-free (SF) graphs. The SW graphs with low ($p = 0.2$) and high ($p = 0.8$) probability of rewiring and mean degree $\langle k \rangle = 6$ are generated via the Watts–Strogatz (WS) algorithm.⁴¹ The SF graph is generated using the Barabási–Albert (BA) algorithm, in which the network is grown by adding a new vertex through attaching $m = 3$ new edges with $n_0 = 3$ existing vertices⁴² that keeps $\langle k \rangle \approx 6$ similarly to SW graphs. These graphs are generated using the `LightGraphs` package for Julia.⁴³ Initial phases θ_i are distributed homogeneously within the range $[0, 2\pi)$.

Below, we report and discuss the principal finding of our study on extreme behavior in the proposed Kuramoto model. We explicitly focus our attention on the macroscopic network behavior and its correlates with the microscopic dynamics of individual units.

A. Macroscopic behavior

First, we explore how the network topology impacts the transition to coherence in the proposed Kuramoto model under excitability resource constraints. We hypothesize that since resource consumption is an internal force that subserves the maintenance of a globally incoherent state, the explosive synchronization, in its turn, should act in the opposite direction, i.e., forcing an abrupt transition to global synchrony. In this regard, we expect that the network topology supporting a discontinuous transition to coherence should establish extreme behavior accordingly.

With this aim, we analyze the macroscopic network dynamics in three types of topology: strongly rewired SW graph ($p = 0.8$, close to a random coupling), weakly rewired SW graph ($p = 0.2$, close to regular non-local coupling), and hierarchical SF graph. Figure 2 reports the main findings. Indeed, in the absence of resource constraints, i.e., $\beta = 0.0$ and $\lambda_i \approx \lambda_0$, $i \in [1, N]$, only the SF network exhibits the first-order explosive transition to coherence following Gómez-Gardenes *et al.*³⁹ At the same time, both SW graphs demonstrate a reversible continuous transition [Fig. 2(a)].

Account of a resource constraint at a rate of $\beta = 0.002$ is presented in Figs. 2(b) and 2(c). The plots in Fig. 2(b) depict the evolution of the histogram $P[R(t)]$ computed after the end of the transient process, $t_{tr} = 10^3$ time units. Figure 2(b) is complemented by the histograms $P[R(t)]$ plotted for specific values of λ_0 in Fig. 2(c). It is seen that in both SW networks under resource constraints, the transition to coherence is smooth and does not show any sign of extreme behavior as the corresponding histograms obey the Weibull distribution throughout the considered range of λ_0 , $p < 0.05$ via a χ^2 -test [left and middle panels in Figs. 2(b) and 2(c)].

In contrast, the SF network under resource constraints exhibits a stable globally incoherent state for low values of $\lambda_0 < 1.4275$, and a globally synchronized ensemble is established for $\lambda_0 > 1.4925$. The intriguing fact is that the SF network establishes an intermediate state—a region of bistability with coexisting globally coherent and

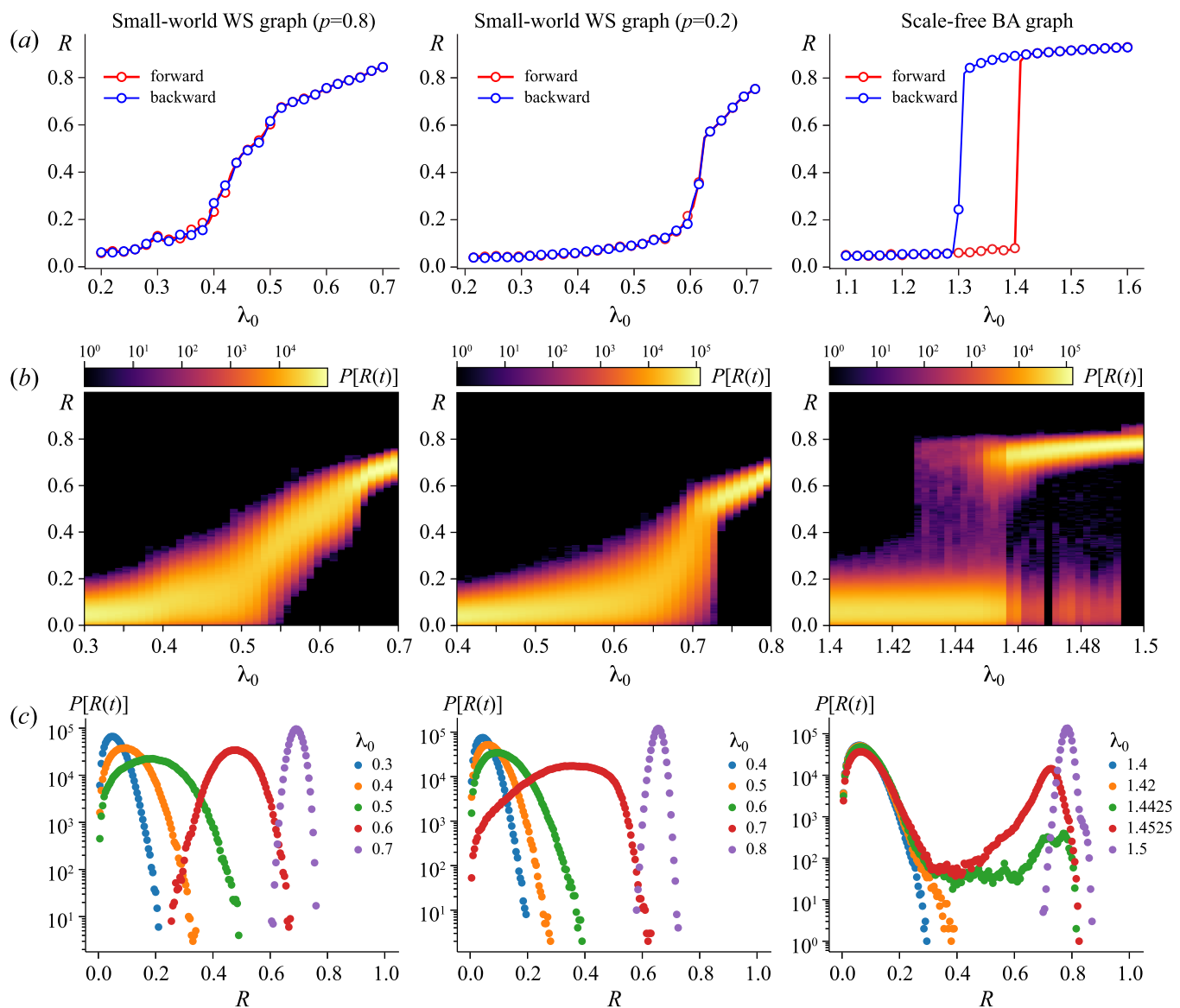


FIG. 2. The impact of network topology on transitions to coherence. The left and middle columns represent the results for strongly ($p = 0.8$) and weakly ($p = 0.2$) rewired SW graph, and the right column depicts the results for the SF graph. (a) Forward (red) and backward (blue) transitions in a conventional Kuramoto model under increasing and decreasing coupling strength λ . (b) Histogram $P(R)$ vs the depth of excitability baths λ_0 in the proposed Kuramoto model under resource constraints. (c) Histograms $P(R)$ in a semi-log scale for fixed values of λ_0 (given in the legend to each plot).

inherent states as the system approaches a tipping point of forward transition, $\lambda_0 \in [1.4275, 1.4925]$ [right panel in Fig. 2(b)]. Notably, the histogram $P[R(t)]$ obeys a Weibull distribution, $p < 0.05$ via a χ^2 -test, only for $\lambda_0 \leq 1.4$ [blue circles in Fig. 2(c), right panel]. Further increase of λ_0 contributes to a developing tail of the Weibull distribution as the system approaches the bistability area [orange circles in the right panel of Fig. 2(c)]. Entering the area of bistability, the histogram $P[R(t)]$ demonstrates a dragon-king-like distribution^{44–46}

characterized by a pronounced peaking exceedance at $R \approx 0.75$ [green circles in the right panel of Fig. 2(c)]. This peak signs the emergence of extreme events associated with rare and short-living states of global synchronization. Under the growth of the resource bath depth λ_0 , the distribution $P[R(t)]$ becomes bimodal that indicates developed bistability, where both coherent and incoherent states are almost equally likely [red circles in the right panel of Fig. 2(c)].

Figure 3 reports the macroscopic dynamics of the proposed Kuramoto model under the excitability resource constraints depicted through the time-series of global order parameter $R(t)$ and corresponding phase trajectories on the $(\langle \lambda \rangle, R)$ -plane for the characteristic values of λ_0 . At low λ_0 , the system exhibits a turbulent drift in the neighborhood of a fixed point—a single stable attractor [Fig. 3(a)]. At the entrance of the bistability region, the system demonstrates rare short-living extreme synchronization events

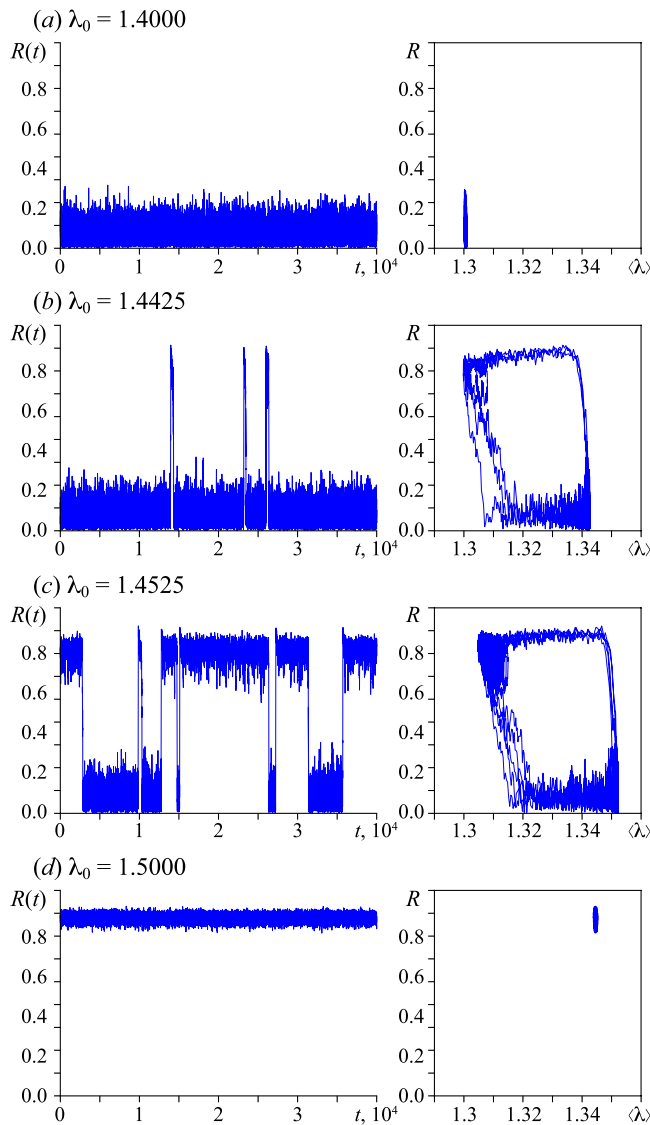


FIG. 3. Macroscopic behavior of the SF network under excitability resource constraints. The left and right columns present time dependencies of global order parameter $R(t)$ and corresponding phase trajectories in the state space $(\langle \lambda \rangle, R)$, respectively, for different values of excitability bath depth λ_0 : (a) $\lambda_0 = 1.4000$, (b) $\lambda_0 = 1.4425$, (c) $\lambda_0 = 1.4525$, and (d) $\lambda_0 = 1.5000$.

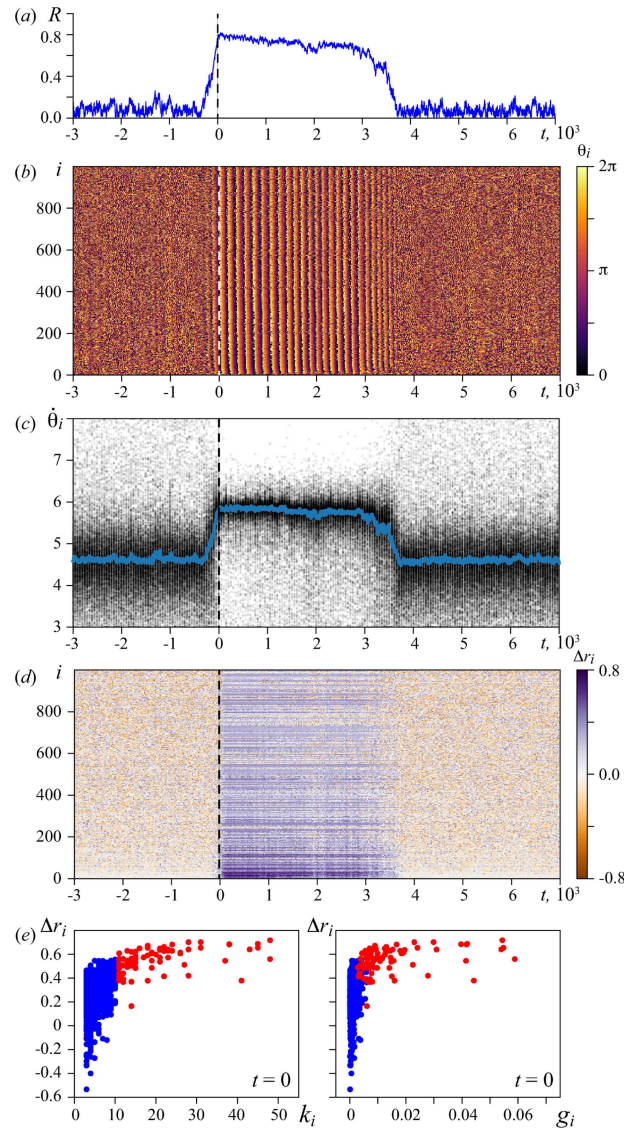


FIG. 4. Microscopic dynamics of the SF network under excitability resource constraints during a single extreme event. The plots are obtained for $\lambda_0 = 1.4425$. (a) Time dependence of the global order parameter $R(t)$. (b) Space-time plot of the instantaneous phase θ_i (black dots) and average frequency $\langle \dot{\theta}_i \rangle$ (blue solid line). (c) Distribution of the instantaneous angular velocity $\dot{\theta}_i$ (black dots) and average frequency $\langle \dot{\theta}_i \rangle$ (blue solid line). (d) Space-time plot of the normalized local order parameter Δr_i . Vertical dashed lines indicate the transition to global coherence. (e) Scatterplots show the normalized local order parameter vs node's degree $\Delta r_i(k_i)$ (left) and node's betweenness centrality $\Delta r_i(g_i)$ (right) at $t = 0$, respectively. Here, red circles indicate highly connected units ($k_i > 10$), and blue circles depict the remaining network nodes.

[Fig. 3(b)]. In this case, the two attractors—a stable fixed point (incoherence) and an unstable fixed point (global coherence)—coexist and are reachable for the system. As the system has enough excitability resources, it sharply leaves a stable fixed point basin and

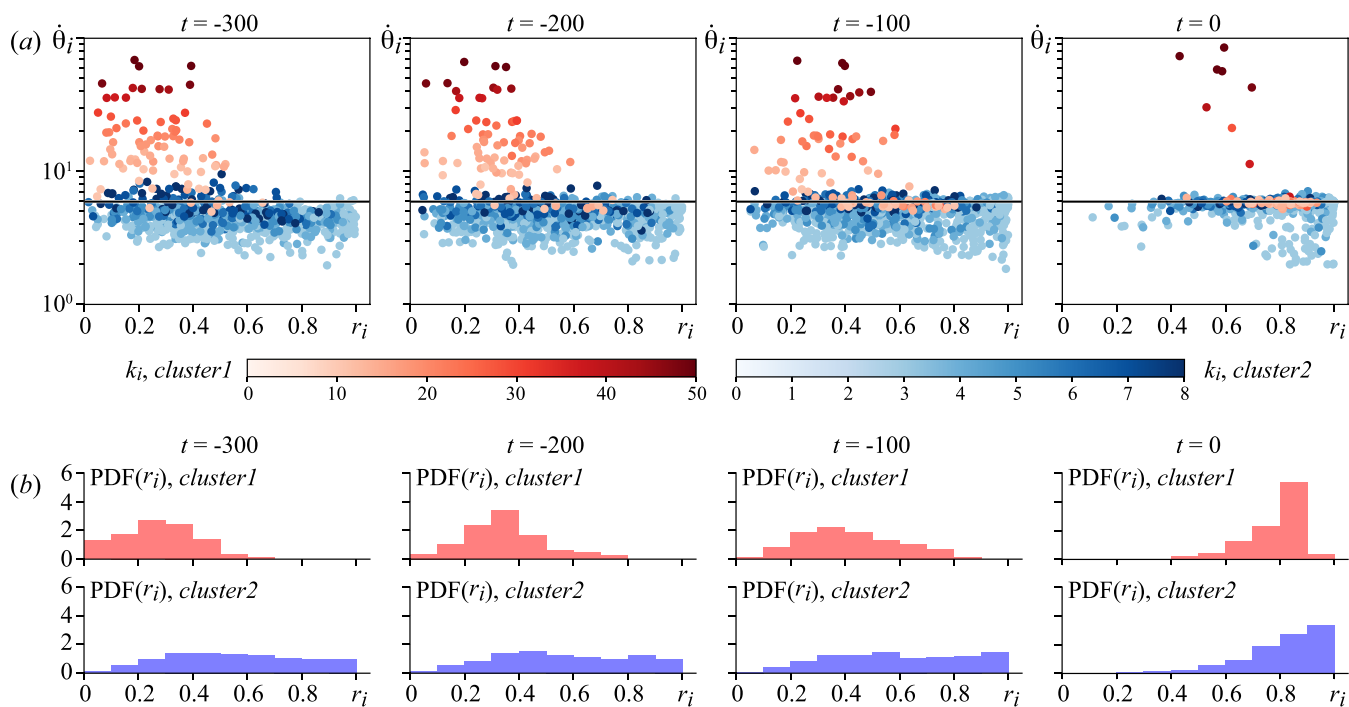


FIG. 5. Mechanism of the extreme synchronization event onset. Columns from left to right depict the network dynamics approaching extreme synchronization event onset at $\lambda_0 = 1.4425$. (a) Distributions of the network units on the plane $(r_i, \dot{\theta}_i)$. Here, the circles are color-coded by the value of node's degree k_i in shades of red for highly connected units and in shades of blue for the remaining ones. The horizontal black line indicates the main frequency $\Omega = \langle \omega_i \rangle = \langle k_i \rangle \approx 6$. (b) Corresponding PDFs of the local order parameter r_i for highly connected nodes (top panels, red bars) and the remaining nodes (bottom panels, blue bars).

approaches the unstable fixed point. However, the network resource is insufficient to stay in the neighborhood of an unstable fixed point; therefore, the phase trajectory goes around the unstable attractor and returns to a stable one. In the case of developed bistability, the network continuously switches between the coherent and incoherent states; i.e., a two-state intermittency is established [Fig. 3(c)]. The system has a sufficient amount of resources to enter the basin of the attractor associated with the global network coherence and to stay there for a finite time interval. However, the system occasionally exits the attractor of global coherence under the sudden deficit of resource and, thus, drifts between the coherent and incoherent states consuming and recovering its resource. Finally, a large amount of resource stored in the bath leads to trivial dynamics—the vanishing of the fixed point determining the incoherent drift; therefore, the system converges to the only possible state of global coherence [Fig. 3(d)].

Since the main focus of the current study is devoted explicitly to the extreme behavior in a proposed Kuramoto model, we proceed with the analysis of microscopic dynamics underlying the transition to synchronization events.

B. Microscopic dynamics

Figure 4 illustrates the dynamics of the Kuramoto oscillators' ensemble under resource constraints during a single rare synchronization event at $\lambda_0 = 1.4425$. For convenience, the network units

are ordered in descending order of their degree in the space-time plots. The time-series of global order parameter $R(t)$ in the course of this event is shown in Fig. 4(a). It is seen from Fig. 4(b) that the majority of the network nodes undergoes an abrupt transition from incoherent drift to coherence, remains phase-locked throughout the event, and gradually leaves the synchronized cluster. As expected, Fig. 4(c) shows that throughout an extreme event, the angular velocities of the network units group near the main frequency, which is the mean natural frequency or, equivalently, mean degree: $\Omega = \langle \omega_i \rangle = \langle k_i \rangle \approx 6$. To characterize better the involvement of the individual units in a synchronization event, we introduce a normalized local order parameter $\Delta r_i = r_i - \langle r_i \rangle_{pre}$, where $\langle r_i \rangle_{pre}$ is a mean local order parameter calculated over the time frame from -3×10^3 to -1×10^3 time units preceding the event. Figure 4(d) demonstrates that the most interconnected nodes exhibit a greater increase of the local order parameter, colored in dark purple, concerning a preceding turbulent behavior.

Based on the latter, we conclude that the microscopic topological properties of individual nodes determine their involvement and impact on the transition to global coherence. To clarify this issue, we consider the normalized local order parameter vs the units' degree k_i and betweenness centrality g_i at the beginning of synchronization $t = 0$ presented in the left and right panels in Fig. 4(e), respectively. One can see that the high degree/centrality units could be visually dissociated from the bulk of low-degree/centrality nodes. Thus, we separate the entire ensemble into two clusters based on their degree:

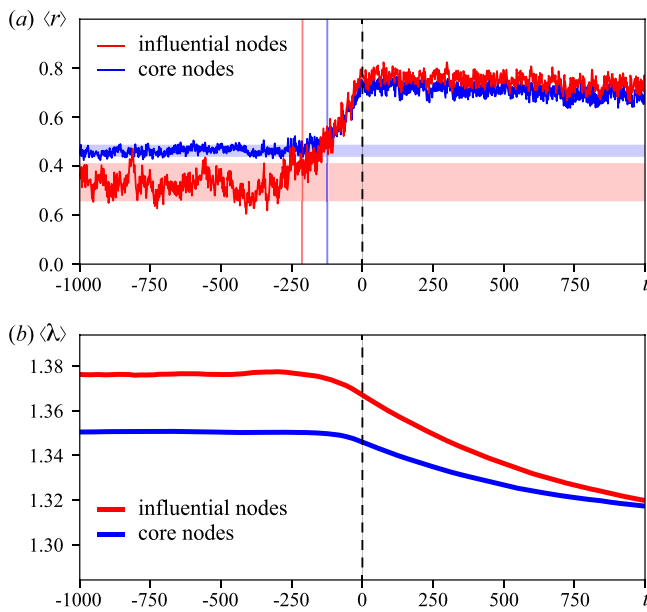


FIG. 6. Synchronization of the influential and core network nodes. Plots (a) and (b) show the time dependencies of local order parameter $\langle r \rangle$ and excitability $\langle \lambda \rangle$ averaged over the influential (red curves) and core network nodes (blue nodes). Shadings of the corresponding color highlight a 95% confidence interval of the mean local order parameter associated with turbulent behavior. A vertical dashed line indicates the transition to global coherence. Vertical solid lines indicate the approximate time moments of synchronization onset for influential (red) and core nodes (blue).

cluster1 comprised the nodes with $k_i \geq 10$ [red dots in Fig. 4(e)] and *cluster2* is composed of the nodes with $k_i < 10$ [blue dots in Fig. 4(e)].

It is important to emphasize that the network units are well-dissociated on the parameter planes formed by the quantifiers of both their *dynamics*—normalized local order parameter Δr_i —and *topology*—nodes' degree k_i and centrality g_i . It is also notable that the node's centrality is useful in unit discrimination as the node's degree. Taken together, these findings imply that the mechanisms of transition to rare synchronization events are determined by the dynamics of interaction between the hierarchically organized layers of the SF network.

To understand the role of particular network nodes in the birth of an extreme synchronization event, we explore the collective behavior of the network approaching a transition to coherence. Figure 5(a) illustrates the snapshots of the node distribution on (r_i, θ_i) -plane color-coded by the value of degree k_i . The snapshots are supplemented with the corresponding PDFs of the local order parameter r_i in both considered clusters [Fig. 5(b)]. In the turbulent state, $t = -300$, the high degree nodes (*cluster1*) are characterized by the low level of local coherence and lie far from the main frequency of the ensemble. In contrast, the network's dynamics are governed by the peripheral low-degree units and their communities (*cluster2*) exhibiting high local synchronization. Thus, the main frequency of the oscillations in the turbulent state is determined

by a large number of small locally coherent groups formed around these units whose degree lies between 4 and 6. Moreover, due to resource constraints, the coherence of these local ensembles is not maintained permanently. These local populations alternately gain and lose coherence being globally desynchronized with each other. We conclude that the peripheral low-degree ensembles act as turbulent active media in the vicinity of a critical point supporting a rapid transition to global coherence. Due to their role in the network dynamics and the population size, we refer them to as the “core” nodes.

However, the transition to coherence is not induced by the interaction of the “core” units. Alternatively, it starts when a sufficient number of units from *cluster1* becomes frequency-locked near the main frequency $\theta_i \approx \Omega$. It is seen that the highest degree nodes from *cluster1* remain desynchronized due to a strong mismatch between their natural frequencies and the main frequency $\Omega \approx 6$. The most important contribution to the transition to coherence is made by the nodes, whose degree is between 10 and 15, i.e., the nodes occupying an intermediate position in the network hierarchy. Due to a relative closeness of their natural frequencies and broad coverage of peripheral units, these nodes have a significant impact on the network's dynamics. At a given value of excitability resource store λ_0 , they establish local coherence within their neighborhood starting an avalanche-like phase-locking of a large number of small peripheral ensembles. Thus, the principal role of these oscillators is a coordination of the distributed local populations to achieve global coherence. We refer to this group of network units as “influential” nodes.

Finally, to emphasize the functional distinction of the “core” and “influential” units, we consider their dynamics near the transition point $t = 0$. Figure 6 shows the time-series of averaged local order parameter $\langle r \rangle$ (a) and averaged excitability $\langle \lambda \rangle$ (b) for each group of network nodes. We see that local coherence in the turbulent state before the transition to coherence is higher in the “core” ensemble than in “influential” units. It coincides with the previous observations and implies the optimal network state from the viewpoint of the resource demands. The synchronization onset starts at $t \approx -250$ as the influential units experience the growth of local coherence and leave the turbulent state. Notably, at the same time, the core nodes stay in their turbulent state and leave it later under the impact of influential nodes at $t \approx -125$. From now on, these populations approach the global coherence together through a sharp growth of local synchrony. At the same time, the averaged excitability level $\langle \lambda \rangle$ in both groups slowly decreases during the onset of an extreme event. Just like the local coherence, the decrease of an excitability level starts earlier in “influential” units, indicating the leading role of this population in the transition to synchronization.

IV. CONCLUSION

To summarize, in the current paper, we propose a self-consistent network model establishing generation of extreme synchronization events. Our model is based on the interaction of paradigmatic Kuramoto phase oscillators under excitability resource constraints. We have explicitly demonstrated that the extreme behavior in such a model is possible due to the interplay between resource consumption and explosive transitions. The latter provides

a hysteresis area, i.e., a region, where the excitation of the coherent and incoherent states is possible, along with the mechanism of a jump-like switching between them. The opposition between the avalanche-like explosive transition to coherence and resource constraints forcing the network to converge to incoherence gives birth to the rare and short-living states of global synchrony. Importantly, the transition to extreme synchronization events is forced mainly by the units occupying medium levels in the network's hierarchy, which we refer to as the "influential" nodes.

Although our observations are limited to the explosive transitions induced by the structure and degree-dependent natural frequencies of the interacting oscillators, we expect that the extreme synchronization events should be excited under the other mechanisms underlying the explosive transitions, i.e., introducing adaptive coupling,^{47,48} multiplexing,^{49–52} frequency displacement,⁵³ etc.

We also expect that the proposed phenomenological model is of potential interest in understanding the complex dynamics of real-world networked systems. Primarily, we assume that the presented results could be relevant in the studies of brain diseases characterized by abnormal synchronization of neural ensembles such as various forms of epilepsy.⁵⁴ Many recent papers show that the formation of epileptic events carries features of extreme behavior,^{34–37} which has been shown for both different animal models of epilepsy^{35,36} and human patients.³⁷ Despite the relative simplicity, our model reflects several properties of epileptic seizures, e.g., an abrupt increase of the main frequency at the beginning of synchronization and its decrease throughout the event (see, for example, Refs. 55 and 56), along with the presence of focal nodes inducing the transition to coherence. We believe that further studies aimed at improving the current model and bringing its properties closer to the real neuronal ensembles will contribute to the modeling and gaining deeper insight into the dynamics behind abnormal epileptic activity.

DEDICATION

With this work, we would like to honor the memory of Professor Vadim S. Anishchenko—outstanding researcher and recognized expert in nonlinear dynamics and complex network theory.

ACKNOWLEDGMENTS

This work was supported by the Russian Foundation for Basic Research (Grant No. 19-52-45026). A.H. acknowledges the President Program of Leading Russian Scientific School Support (Grant No. NSH-2594.2020.2).

DATA AVAILABILITY

The data that support the findings of this study are available within the article.

REFERENCES

- ¹V. Anishchenko, *Complex Oscillations in Simple Systems* (Nauka, 1990).
- ²V. Anishchenko, V. Astakhov, A. Neiman, T. Vadivasova, and L. Schimansky-Geier, *Nonlinear Dynamics of Chaotic and Stochastic Systems: Tutorial and Modern Developments* (Springer Science & Business Media, 2007).
- ³S. A. Bogomolov, A. V. Slepnev, G. I. Strelkova, E. Schöll, and V. S. Anishchenko, *Commun. Nonlinear Sci. Numer. Simul.* **43**, 25 (2017).

- ⁴A. Bukh, E. Rybalova, N. Semenova, G. Strelkova, and V. Anishchenko, *Chaos* **27**, 111102 (2017).
- ⁵E. Rybalova, T. Vadivasova, G. Strelkova, V. S. Anishchenko, and A. Zakharova, *Chaos* **29**, 033134 (2019).
- ⁶S. Boccaletti, V. Latora, Y. Moreno, M. Chavez, and D.-U. Hwang, *Phys. Rep.* **424**, 175 (2006).
- ⁷A. Arenas, A. Diaz-Guilera, J. Kurths, Y. Moreno, and C. Zhou, *Phys. Rep.* **469**, 93 (2008).
- ⁸S. Boccaletti, A. N. Pisarchik, C. I. Del Genio, and A. Amann, *Synchronization: From Coupled Systems to Complex Networks* (Cambridge University Press, 2018).
- ⁹K. Niizeki, K. Kawahara, and Y. Miyamoto, *J. Appl. Physiol.* **75**, 1815 (1993).
- ¹⁰C. Schäfer, M. G. Rosenblum, H.-H. Abel, and J. Kurths, *Phys. Rev. E* **60**, 857 (1999).
- ¹¹T. Penzel *et al.*, *Front. Physiol.* **7**, 460 (2016).
- ¹²M. Perc *et al.*, *Phys. Rep.* **687**, 1 (2017).
- ¹³M. Rohden, A. Sorge, M. Timme, and D. Witthaut, *Phys. Rev. Lett.* **109**, 064101 (2012).
- ¹⁴A. E. Motter, S. A. Myers, M. Anghel, and T. Nishikawa, *Nat. Phys.* **9**, 191 (2013).
- ¹⁵P. Fries, *Neuron* **88**, 220 (2015).
- ¹⁶V. A. Maksimenko *et al.*, *Front. Behav. Neurosci.* **13**, 220 (2019).
- ¹⁷N. Frolov, V. Maksimenko, and A. Hramov, *Chaos* **30**, 121108 (2020).
- ¹⁸F. Mormann, K. Lehnertz, P. David, and C. E. Elger, *Physica D* **144**, 358 (2000).
- ¹⁹K. Lehnertz *et al.*, *J. Neurosci. Methods* **183**, 42 (2009).
- ²⁰A. Lüttjohann and G. van Luijtelaar, *Front. Physiol.* **6**, 16 (2015).
- ²¹N. Frolov, V. Maksimenko, A. Lüttjohann, A. Koronovskii, and A. Hramov, *Chaos* **29**, 091101 (2019).
- ²²C. J. Stam, *Nat. Rev. Neurosci.* **15**, 683 (2014).
- ²³T. M. Medvedeva, M. V. Sysoeva, G. van Luijtelaar, and I. V. Sysoev, *Neural Netw.* **98**, 271 (2018).
- ²⁴T. Medvedeva, M. Sysoeva, A. Lüttjohann, G. van Luijtelaar, and I. Sysoev, *PLoS One* **15**, e0239125 (2020).
- ²⁵A. Rothkegel and K. Lehnertz, *Europhys. Lett.* **105**, 30003 (2014).
- ²⁶A. Rothkegel and K. Lehnertz, *New J. Phys.* **16**, 055006 (2014).
- ²⁷R. Karnatak, G. Ansmann, U. Feudel, and K. Lehnertz, *Phys. Rev. E* **90**, 022917 (2014).
- ²⁸G. Ansmann, K. Lehnertz, and U. Feudel, *Phys. Rev. X* **6**, 011030 (2016).
- ²⁹M. Gerster *et al.*, *Chaos* **30**, 123130 (2020).
- ³⁰W. A. Catterall, *Science* **223**, 653 (1984).
- ³¹V. Wimmer, H. Lester, and S. Petrou, "Ion channels—Ion channel mutations in familial epilepsy," in *Encyclopedia of Basic Epilepsy Research*, edited by P. A. Schwartzkroin (Academic Press, Oxford, 2009), pp. 651–658.
- ³²K. A. Wiley, P. J. Mucha, and D. S. Bassett, "Synchronization of coupled Kuramoto oscillators under resource constraints," arXiv preprint [arXiv:2002.04092](https://arxiv.org/abs/2002.04092) (2020).
- ³³Y. Zhang and S. H. Strogatz, "Designing temporal networks that synchronize under resource constraints," [arXiv:2101.02721](https://arxiv.org/abs/2101.02721) (2021).
- ³⁴K. Lehnertz, "Epilepsy: Extreme events in the human brain," in *Extreme Events in Nature and Society* (Springer, 2006), pp. 123–143.
- ³⁵A. Pisarchik *et al.*, *Eur. Phys. J. Spec. Top.* **227**, 921 (2018).
- ³⁶N. S. Frolov *et al.*, *Sci. Rep.* **9**, 7243 (2019).
- ³⁷O. E. Karpov *et al.*, *Phys. Rev. E* **103**, 022310 (2021).
- ³⁸S. Boccaletti *et al.*, *Phys. Rep.* **660**, 1 (2016).
- ³⁹J. Gómez-Gardenes, S. Gómez, A. Arenas, and Y. Moreno, *Phys. Rev. Lett.* **106**, 128701 (2011).
- ⁴⁰C. Rackauckas and Q. Nie, *J. Open Res. Softw.* **5**, 15 (2017).
- ⁴¹D. J. Watts and S. H. Strogatz, *Nature* **393**, 440 (1998).
- ⁴²A.-L. Barabási and R. Albert, *Science* **286**, 509 (1999).
- ⁴³J. F. Seth Bromberger *et al.* JuliaGraphs/LightGraphs.jl: An optimized graphs package for the Julia programming language, 2017.
- ⁴⁴D. Sornette and G. Ouillon, *Eur. Phys. J. Spec. Top.* **205**, 1 (2012).
- ⁴⁵C. Ancey, *Eur. Phys. J. Spec. Top.* **205**, 117 (2012).
- ⁴⁶A. Mishra *et al.*, *Phys. Rev. E* **97**, 062311 (2018).
- ⁴⁷X. Zhang, S. Boccaletti, S. Guan, and Z. Liu, *Phys. Rev. Lett.* **114**, 038701 (2015).

- ⁴⁸M. M. Danziger, I. Bonamassa, S. Boccaletti, and S. Havlin, *Nat. Phys.* **15**, 178 (2019).
- ⁴⁹S. Jalan, V. Rathore, A. D. Kachhvah, and A. Yadav, *Phys. Rev. E* **99**, 062305 (2019).
- ⁵⁰A. Kumar, S. Jalan, and A. D. Kachhvah, *Phys. Rev. Res.* **2**, 023259 (2020).
- ⁵¹P. Khanra, P. Kundu, C. Hens, and P. Pal, *Phys. Rev. E* **98**, 052315 (2018).
- ⁵²N. Frolov *et al.*, *Chaos, Solitons Fractals* **147**, 110955 (2021).
- ⁵³S. Jalan, A. Kumar, and I. Leyva, *Chaos* **29**, 041102 (2019).
- ⁵⁴S. Kalitzin *et al.*, *Neurobiol. Dis.* **130**, 104488 (2019).
- ⁵⁵E. Sitnikova, A. E. Hramov, A. A. Koronovsky, and G. van Luitelaar, *J. Neurosci. Methods* **180**, 304 (2009).
- ⁵⁶G. Van Luitelaar, A. Hramov, E. Sitnikova, and A. Koronovskii, *Clin. Neurophysiol.* **122**, 687 (2011).